Virtual source for rotational symmetric Lorentz-Gaussian beam

Qiongge Sun (孙琼阁)[1], Ailan Li (李爱兰)[2], Keya Zhou (周可雅)[1], Zhengjun Liu (刘正君)[3], Guangyu Fang (方光宇)[1], and Shutian Liu (刘树田)[1*]

[1]*Department of Physics, Harbin Institute of Technology, Harbin 150001, China*

[2]*College of Electronics and Information Engineering, Beijing City University, Beijing 100083, China*

[3]*Department of Automation Measurement and Control Engineering, Harbin Institute of Technology, Harbin 150001, China*

[*]*Corresponding author: stliu@hit.edu.cn*

Received December 12, 2011; accepted February 13, 2012; posted online March 28, 2012

The virtual source for generation of rotational symmetric Lorentz-Gaussian (RLG) wave whose propagating dynamics present the rotational symmetry is identified. Closed-form expressions, including integral and differential representations, are derived for this kind of Lorentz-Gaussian (LG) wave, thereby yielding paraxial approximation of the RLG beam in the appropriate regime. From the spectral representation of this wave, the first three order corrections of nonparaxial approximations are determined for a corresponding paraxial RLG beam. Moreover, the relationship between the RLG beam and the Hermite-Gaussian beam is revealed.

OCIS codes: 260.2110, 260.1960, 350.5500, 010.3310.

doi: 10.3788/COL201210.062601.

The Lorentz-Gaussian (LG) beams obtained by Gawhary *et al.* as exact solutions of a paraxial wave equation for propagation in optical systems can be described as the product of two independent Lorentz functions apodizated by Gaussian beams and as solution modes in novel laser resonators[1,2]. These beams have been introduced to describe highly divergent beams generated by certain laser sources, such as double-heterojunction $Ga_{1-x}Al_xAs$[3−5]. Thus far, previous work on this type of beam has attracted intensive research and has extended the paraxial regime to the nonparaxial regime[6−12]. For example, based on the vectorial Rayleigh-Sommerfeld integral formula, the analytical propagation equation of a nonparaxial LG beam in free space has been derived[7]. The rotational symmetric LG (RLG) beam with symmetric characteristics of rotation, which can be regarded as a special mathematical model of LG beam, has not yet received much attention.

Because the nonparaxial propagation of optical beams has attracted increasing attention in optics[13], virtual source method, which is first proposed by Deschamps[14] and then systematically developed by Felsen *et al.*[15,16], has been widely applied to investigate the characterization and propagation of beams in and beyond the paraxial regime. Seshadri[17−20] employed this method to derive an integral expression for Bessel-Gaussian, cylindrically symmetric elegant Laguerre-Gaussian, fundamental Gaussian[21], and elegant Hermite-Gaussian beams. Bandres *et al.* applied this method to determine a higher-order complex source of elegant Laguerre-Gaussian wave with angular mode number m and radial mode number n[22]. Zhang *et al.* extended this method to generate a cosh-Gaussian wave with four complex virtual sources[23], whereas Deng *et al.* derived a higher-order complex virtual source for the elegant Hermite-Laguerre-Gaussian wave[24]. Based on the operator transformation technique, the multiple complex point sources required to generate a coherent superposition of waves have also been introduced[25]. A group of virtual sources that generate a hollow Gaussian wave based on the superposition of beams has been generated[26]. However, to the best of our knowledge, the virtual source of the RLG beam has not been investigated. The exact solution of the RLG wave, including integral and differential representations, has also not been reported.

In this letter, based on the superposition of beams, a virtual source for the RLG wave ($\omega_0 = \sqrt{2}\omega_{0x} = \sqrt{2}\omega_{0y}$) is studied. The expression of exact solution is obtained for this wave. From this expression, the paraxial approximation and nonparaxial corrections of all orders can be determined for this RLG beam.

Suppose $\mathrm{LG}(x, y, z)$ to be a monochromatic paraxial scalar wave function that denotes a paraxial LG wave propagating along the positive z axis. The ordinary LG field at the original plane ($z = 0$) is characterized by

$$\mathrm{LG}(x,y,0) = \frac{A}{\omega_{0x}\omega_{0y}} \frac{1}{[1+(x/x\omega_{0x})^2]} \frac{1}{[1+(y/\omega_{0y})^2]} \cdot \exp\left(-\frac{x^2+y^2}{\omega_0^2}\right), \tag{1}$$

where ω_{0j} ($j = x, y$) and ω_0 are parameters related to the beam width and A is a constant value. Here, A, ω_{0x}, ω_{0y}, and $\omega_0 \in \Re$. The Lorentz distribution has been expanded in terms of the elements of the complete orthonormal basis set of the Hermite-Gaussian functions[27]. The expansion is given by[27−29]

$$\mathrm{LG}(x,y,0) = \frac{A\pi}{2\omega_{0x}\omega_{0y}} \sum_{m=0}^{\infty}\sum_{n=0}^{\infty} a_{2m}a_{2n}H_{2m}(x/\omega_{0x}) \cdot H_{2n}(y/\omega_{0y}) \exp\left[-\frac{x^2}{\omega_x^2} - \frac{y^2}{\omega_y^2}\right], \tag{2}$$

$$1/\omega_j^2 = 1\omega_0^2 + 1/2\omega_{0j}^2, \tag{3}$$

where a_{2m} and a_{2n} are adjustable functions with adjustable parameters that are used to obtain reasonably convergent results, especially when only a limited number of terms is used in the expansion, and H_{2m} and H_{2n} are Hermite polynomials of even order. The values of a_{2m} and a_{2n} are listed in Ref. [27]. Supposing that $\omega_{0j} = \omega_j = \omega$, we obtain the waist of the Gaussian part $\omega_0 = \sqrt{2}\omega$ in Eq. (1). We adopt the same beam widths of the Lorentz part in the x and y directions. The Lorentz part is modulated by Gaussian part with the appropriate waist, leading to the RLG beam, which presents a nearly round spot in original plane. After applying the beam width relation, the expansion equation of LG beams on basis of Hermite-Gaussian functions (Eq. (2)) can be rewritten as the RLG beams:

$$\mathrm{RLG}(x,y,0) = \frac{A\pi}{2\omega^2}\sum_{m=0}^{\infty}\sum_{n=0}^{\infty} a_{2m}a_{2n}H_{2m}\left(\frac{x}{\omega}\right)H_{2n}\left(\frac{y}{\omega}\right) \cdot \exp\left[-\frac{x^2+y^2}{\omega^2}\right]. \quad (4)$$

Equation (4) stands for LG beam with rotational symmetry, which presents a nearly round spot in the original plane. That is to say, the RLG beams present the symmetric characteristic in original plane, and can be obtained by means of the superposition of even-order Hermite-Gaussian beams.

We display the propagation dynamics of the RLG wave in free space by means of the Fresnel diffraction method in Fig. 1. The chosen planes are $z = 0.5z_{\mathrm{R}}$, z_{R}, and $2z_{\mathrm{R}}$, where z_{R} stands for the Rayleigh distance. Normalized intensity distributions at the chosen planes for the approximated version of RLG wave are also plotted in Fig. 1 for comparison. Clearly, the RLG wave presents a prominent symmetrical characteristic different from the ordinary LG wave. Moreover, Figs. 1(a) and (d) show that the intensity distribution of the RLG beam is the same as that of its approximated version at the $z = 0.5z_{\mathrm{R}}$ plane. Figures 1(b) and (e) also present the intensity distribution of these two beams at the $z = z_{\mathrm{R}}$ plane. Clearly, the intensity distribution patterns of these beams

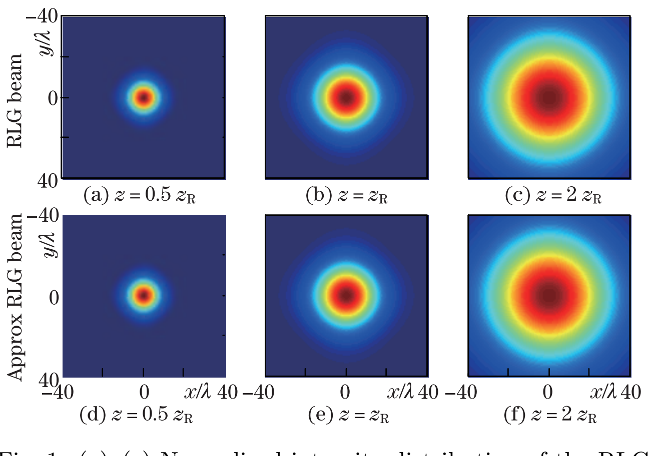

Fig. 1. (a)–(c) Normalized intensity distribution of the RLG beam at different transverse sections (x/λ, y/λ). (d)–(f) Approximated version of the intensity distribution by means of Hermite-Gaussian functions (x/λ, y/λ). Simulation is performed for $\lambda = 1$ μm and $\omega = 20$ μm. All the graphs cover the range [–40,40]×[–40,40].

at the $z = z_{\mathrm{R}}$ plane, as well as at the $z = 2z_{\mathrm{R}}$ plane, are the same. Roughly speaking, the superposition of the even-order Hermite-Gaussian beams can stand for the RLG beam, not only at the original plane, but also at the arbitrary section on propagation in and beyond the Rayleigh distance.

In the Cartesian coordinate system, the beam is assumed to be generated by a higher-order point source with the intensity of S_{ex} situated at $z = z_{ex}$. We also assume that the proper choice of S_{ex} and z_{ex} yields the desired LG beams in the physical space $z > 0$. The wave function satisfies the inhomogeneous Helmholtz equation

$$(\nabla^2 + k^2)\mathrm{RLG}(x,y,z) = -S_{ex}T_{mn}(\partial_x^2, \partial_y^2)\delta(x)\delta(y) \cdot \delta(z - z_{ex}), \quad (5)$$

$$T_{mn}(\partial_x^2, \partial_y^2) = \sum_{m=0}^{\infty}\sum_{n=0}^{\infty} \partial_x^{2m}\partial_y^{2n}, \quad (6)$$

where $\nabla^2 = \partial_x^2 + \partial_y^2 + \partial_z^2$ with $\partial_r = \partial/\partial r$ $(r = x, y, z)$. Applying the Fourier transform pairs,

$$\mathrm{RLG}\,(x,y,z) = \iint_{\infty} \widetilde{\mathrm{RLG}}(p_x, p_y, z) \cdot \exp[-\mathrm{i}2\pi(p_x x + p_y y)]\mathrm{d}p_x\mathrm{d}p_y, \quad (7)$$

$$\widetilde{\mathrm{RLG}}(p_x, p_y, z) = \iint_{\infty} \mathrm{RLG}(x,y,z) \cdot \exp[\mathrm{i}2\pi(p_x x + p_y y)]\mathrm{d}x\mathrm{d}y, \quad (8)$$

where p_x and p_y are spatial frequencies in the x and y directions, respectively, and the spatial frequency is $p = (p_x^2 + p_y^2)^{1/2}$. From Eq. (8), $\widetilde{\mathrm{RLG}}(p_x, p_y, z)$ is determined. When the solution of $\widetilde{\mathrm{RLG}}(p_x, p_y, z)$ is substituted into Eq. (7), we obtain

$$\mathrm{RLG}(x,y,z) = \iint_{\infty}\sum_{m=0}^{\infty}\sum_{n=0}^{\infty}\frac{\mathrm{i}S_{ex}}{2\zeta}\exp[\mathrm{i}\zeta(z - z_{ex})] \cdot \exp[-2\pi\mathrm{i}(xp_x + yp_y)](-2\pi\mathrm{i}p_x)^{2m}(-2\pi\mathrm{i}p_y)^{2n}\mathrm{d}p_x\mathrm{d}p_y, \quad (9)$$

for $\mathrm{Re}(z - z_{ex}) > 0$, where $\zeta = [k^2 - 4\pi^2(p_x^2 + p_y^2)]^{1/2}$. The integral of Eq. (9) is rearranged to extend from $-\infty$ to $+\infty$, and the domains of p_x and p_y are extended to complex values. Here, $\widetilde{\mathrm{RLG}}(p_x, p_y, z)$ is an analytic function of complex variable $4\pi^2(p_x^2 + p_y^2)$. This radiation condition is used to select the appropriate branch of ζ.

To obtain a nearly planar wave, we evaluate the integral in Eq. (9) asymptotically. If $4\pi^2(p_x^2 + p_y^2)$ corresponding to the saddle point is smaller than k^2, we expand ζ for small $4\pi^2(p_x^2 + p_y^2)$ and retain the leading term for the amplitude factor and the first two terms for the phase factor. Expanding ζ into a series and keeping the first and second terms, we obtain $\zeta \approx k(1 - 2\pi^2 p^2/k^2)$. Under paraxial approximation $4\pi^2(p_x^2 + p_y^2) \ll k^2$, we replace ζ of the phase factor in Eq. (4) with the first two terms and the amplitude factor with the leading term k. The integrals in Eq. (4) can be evaluated as

$$\mathrm{RLG}(x,y,z)=\frac{\mathrm{i}\exp[\mathrm{i}k(z-z_{ex})]}{2k}\iint\limits_{\infty}\sum_{m=0}^{\infty}\sum_{n=0}^{\infty}S_{ex}\cdot\exp[-2\pi\mathrm{i}(xp_x+yp_y)](-2\pi\mathrm{i}p_x)^{2m}(-2\pi\mathrm{i}p_y)^{2n}\cdot\exp\left[-\mathrm{i}\frac{2\pi^2}{k}(p_x^2+p_y^2)(z-z_{ex})\right]\mathrm{d}p_x\mathrm{d}p_y, \quad (10)$$

$$\mathrm{RLG}(x,y,z)=\exp(\mathrm{i}kz)\sum_{m=0}^{\infty}\sum_{n=0}^{\infty}\partial_x^{2m}\partial_y^{2n}\cdot\left\{\frac{S_{ex}\exp(-\mathrm{i}kz_{ex})}{4\pi(z-z_{ex})}\exp\left[\frac{\mathrm{i}k(x^2+y^2)}{2(z-z_{ex})}\right]\right\}. \quad (11)$$

In order to generate the RLG beam for $z>0$, the input distribution is given by Eq. (4) for boundary condition $z=0$. Because the Hermite Gaussian function is

$$H_m(v)=(-1)^m\exp(v^2)(\mathrm{d}^m/\mathrm{d}v^m)[\exp(-v^2)], \quad (12)$$

by comparing Eqs. (4) and (11) under the boundary condition and applying Eq. (12), the parameters z_{ex} and S_{ex} are determined by the requirement that $\mathrm{RLG}(x,y,z)$ given by Eq. (11) for $z=0$ is reduced to $\mathrm{RLG}(x,y,0)$ in Eq. (4). The result yields

$$z_{ex}=\mathrm{i}\frac{k\omega^2}{2}=\mathrm{i}b, \quad (13)$$

$$S_{ex}=-2A\pi^2\mathrm{i}b\exp(-kb)\sum_{m=0}^{\infty}\sum_{n=0}^{\infty}a_{2m}a_{2n}\omega^{4(m+n)-2}. \quad (14)$$

Then, Eq. (11) will be the paraxial RLG beam

$$\mathrm{RLG}(x,y,z)=\frac{A\pi}{2\omega^2}\exp(\mathrm{i}kz)\sum_{m=0}^{\infty}\sum_{n=0}^{\infty}a_{2m}a_{2n}q(z)^{4(m+n)+2}\cdot H_{2m}\left[\frac{q(z)}{\omega}x\right]H_{2n}\left[\frac{q(z)}{\omega}y\right]\exp\left[-\frac{q^2(z)}{\omega^2}(x^2+y^2)\right], \quad (15)$$

with

$$q^2(z)=(1+\mathrm{i}z/b)^{-1}. \quad (16)$$

As the above equations show, to a given beam width ω, a group of corresponding even-order Hermite-Gaussian beams will compose the LG beam. That is to say, the RLG beam expressed in Eq. (4) can be regarded as the sum of even-order Hermite-Gaussian beams with the same beam width ω.

By applying Eqs. (13) and (14), one can also obtain the exact solution of the inhomogeneous Helmholtz equation in the integral representation from Eq. (9):

$$\mathrm{RLG}(x,y,z)=A\pi^2b\omega^{4(m+n)^{-2}}\exp(-kb)\sum_{m=0}^{\infty}\sum_{n=0}^{\infty}a_{2m}a_{2n}\cdot\iint\limits_{\infty}\frac{\exp[\mathrm{i}\zeta(z-\mathrm{i}b)]}{\zeta}\exp[-2\pi\mathrm{i}(xp_x+yp_y)]\cdot(-2\pi p_x)^{2m}(-2\pi p_y)^{2n}\mathrm{d}p_x\mathrm{d}p_y. \quad (17)$$

The integral representation for the RLG wave is given by Eq. (17). The wave function representing the corresponding paraxial RLG beam is given by Eq. (15). For $z>0$, the solution given by Eq. (17) is the exact solution to the homogeneous equation corresponding to Eq. (5). This exact solution yields the correct paraxial approximation in the appropriate limit that excludes all the nonparaxial contributions, as well as the evanescent waves. All the contributions can be summed up by evaluated the integral in Eq. (17).

By applying the Green-function approach, the differential representation of a RLG wave can be determined. The solution of the differential equation

$$(\nabla^2+k^2)\mathrm{G}(r,z)=-S_{ex}\delta(x)\delta(y)\delta(z-z_{ex}), \quad (18)$$

is given by

$$\mathrm{G}(r,z)=S_{ex}\exp(\mathrm{i}kR)4\pi R, \quad (19)$$

where $R=[x^2+y^2+(z-\mathrm{i}b)^2]^{1/2}$. In applying the operator

$$\widehat{T}=T_{mn}(\partial_x^2,\partial_y^2) \quad (20)$$

from the left in both sides of the Eq. (19) and using Eq. (14), when the result is compared with Eq. (5), the differential or multipole representation of the RLG beam is found to be

$$\mathrm{RLG}(x,y,z)=-\frac{A\pi}{2}\mathrm{i}b\exp(-kb)T_{mn}(\partial_x^2,\partial_y^2)\omega^{4(m+n)-2}\cdot a_{2m}a_{2n}\left[\frac{\exp(\mathrm{i}kR)}{R}\right]. \quad (21)$$

From Eq. (21), we can see that this uniquely shaped LG beam can be generated by applying the operator in Eq. (20) to the complex-source-point spherical wave $S_{ex}\exp(\mathrm{i}kR)/4\pi R$ that corresponds to the paraxial Gaussian beam. When comparing the differential representation of RLG beam with the corresponding representation of Hermite-Gaussian beam (in Ref. [20]), we can see that the main difference is their operators. One applies the operator $\partial_x^m\partial_y^n$ to the complex-source-point spherical wave to generate Hermite-Gaussian beam, whereas the other uses $\sum\limits_{m=0}^{\infty}\sum\limits_{n=0}^{\infty}\partial_x^{2m}\partial_y^{2n}$ to realize the RLG beam. Clearly, the RLG beam can be described as the infinity of even-order Hermite-Gaussian beams, as proven in Eq. (15). However, we can select appropriate adjustable parameters in adjustable functions a_{2m} and a_{2n} to obtain a limited number of terms used in the expansion in practice.

In order to obtain the nonparaxial corrections of the RLG beam, we can perform the series expansion of $1/\zeta$ and $\exp[\mathrm{i}\zeta(z-z_\mathrm{d})]$ in Eq. (17) by using the perturbative series method. The product of both series terms up to order $(k\omega)^{-2j}$ are retained and we can obtain the jth order corrections. By this expansion operation, the first three nonparaxial corrections of RLG beam for $j=3$ can be represented as

$$\mathrm{RLG}(x,y,z)=\frac{A\pi^2}{2}\exp(\mathrm{i}kz)\sum_{m=0}^{\infty}\sum_{n=0}^{\infty}a_{2m}a_{2n}\omega^{4(m+n)}$$

$$\cdot \iint\limits_{\infty} \exp\left[-\frac{\mathrm{i}2\pi^2 p^2}{k}(z-\mathrm{i}bt)\right] G(2\pi p, z)(-2\pi \mathrm{i} p_x)^{2m}$$
$$\cdot (-2\pi \mathrm{i} p_y)^{2n} \exp[-2\pi \mathrm{i}(xp_x + yp_y)]\mathrm{d}p_x \mathrm{d}p_y, \quad (22)$$

where

$$G(\xi, z) = 1 + k^{-2}G_2(\xi, z) + k^{-4}G_4(\xi, z) + k^{-6}G_6(\xi, z), \quad (23)$$

$$G_2(\xi, z) = a_{21}\xi^2 - a_{22}\omega^2 \frac{\xi^4}{q^2(z)}, \quad (24)$$

$$G_4(\xi, z) = a_{42}\xi^4 - a_{43}\omega^2 \frac{\xi^6}{q^2(z)} + a_{44}\omega^4 \frac{\xi^8}{q^4(z)}, \quad (25)$$

$$G_6(\xi, z) = a_{63}\xi^6 - a_{64}\omega^2 \frac{\xi^8}{q^2(z)} + a_{65}\omega^4 \frac{\xi^{10}}{q^4(z)} - a_{66}\omega^6 \frac{\xi^{12}}{q^6(z)}, \quad (26)$$

where $a_{21} = 1/2$, $a_{22} = 1/16$, $a_{42} = 3/8$, $a_{43} = 1/16$, $a_{44} = 1/512$, $a_{63} = 5/16$, $a_{64} = 15/256$, $a_{65} = 3/1\,024$, and $a_{66} = 1/(6 \times 4\,096)$. Together with Eqs. (23)–(26), after we define a dimensionless perturbation parameter $\sigma = 1/(k\omega)$, the integral in Eq. (22) can be evaluated as the nonparaxial RLG beam accurate to any order σ^2.

$$\mathrm{RLG}(x, y, z) = \frac{A\pi}{2\omega^2} \exp(\mathrm{i}kz) \sum_{m=0}^{\infty} \sum_{n=0}^{\infty} a_{2m} a_{2n}$$
$$\cdot [q(z)]^{4(m+n)+2} \exp\left[-\frac{q^2(z)}{\omega^2}(x^2 + y^2)\right]$$
$$\cdot \sum_{j=0}^{3} \sigma^{-2j}(-1)^j q^{2j}(z) f_{m,n}^{(2j)}(x, y, z), \quad (27)$$

where

$$f_{m,n}^{(2j)}(x, y, z) = \sum_{t=j}^{2j} a_{2j,t} \sum_{l=0}^{t} \frac{t!}{l!(t-l)!} H_{2m+2(t-l)} \cdot \left[\frac{q(z)}{\omega}x\right] H_{2n+2l}\left[\frac{q(z)}{\omega}y\right]. \quad (28)$$

Equation (27) represents the nonparaxial expression of the RLG beam taking up to the first three nonparaxial corrections. The above expression indicates that the RLG beam can be described as a superposition of even-order Hermite-Gaussian beams. Clearly, the nonparaxial solution approaches the exact solution as the parameter j increases. Specifically, when the parameter j becomes infinite, the nonparaxial solution becomes the exact solution.

Figure 2 shows the normalized intensity distribution respectively associated with the paraxial RLG beam, the nonparaxial correction solution of the RLG beam, and the corresponding exact solution of the RLG wave at the given plane. The dimensionless perturbation parameter of the simulation is $\sigma = 0.5$. Figure 2 shows that the second-order correction solution is closer to the exact solution than the first-order correction solution at different transverse plane. The paraxial solution, the nonparaxial correction solution, and the exact solution have more obvious discrepancies when the propagation distance is increased because the beam expands the paraxial approximation.

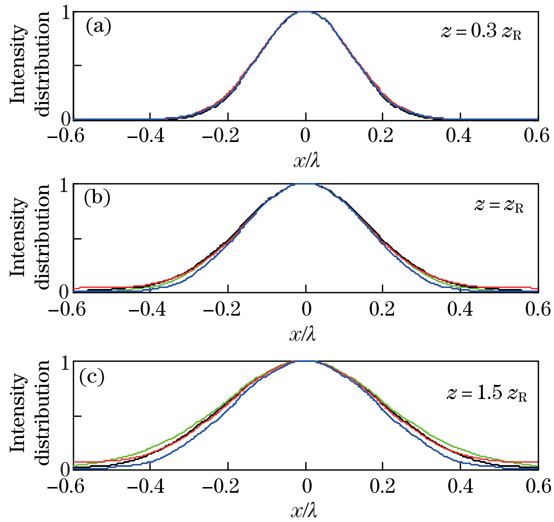

Fig. 2. Comparison of the normalized intensity distribution respectively associated with the paraxial RLG beam (dotted-dashed curve), the first-order (dashed curve) and the second-order (dotted curve) nonparaxial corrections of RLG beam, and the corresponding exact solution of the RLG wave (solid curve) at the given planes. The parameters are $\lambda = 1$ μm and $\sigma = 0.5$.

In conclusion, a complex virtual source required for generation of the RLG beam is presented on the basis of the superposition of beams. The relation between RLG beam and Hermite-Gaussian beam is revealed. We obtain the integral and the differential representations for the RLG beam. From the integral representation of RLG, we derive the first three orders of nonparaxial corrections for the corresponding paraxial RLG beam. Comparisons of the normalized intensity distribution associated with the paraxial RLG beam, the first two nonparaxial corrections of RLG beam, and the exact RLG wave at the given planes are presented numerically.

This work was supported by the National "973" Program of China (No. 2011CB301801), the National Natural Science Foundation of China (Nos. 10974039, 11047153, 10904027, 61008039, and 11104049), and the Doctoral Program of Higher Education (No. 20102302120009).

References

1. O. E. Gawhary and S. Severini, J. Opt. A: Pure Appl. Opt. **8,** 409 (2006).
2. O. E. Gawhary and S. Severini, Opt. Commun. **269,** 274 (2007).
3. A. Naqwi and F. Durst, Appl. Opt. **29,** 1780 (1990).
4. W. P. Dumke, IEEE J. Quantum Electron. **QE-11,** 400 (1975).
5. J. Yang, T. Chen, G. Ding, and X. Yuan, Proc. SPIE **6824,** 68240A (2007).
6. G. Zhou, Appl. Phys. B **93,** 891 (2008).
7. G. Zhou, J. Opt. Soc. Am. B **26,** 141 (2009).
8. G Zhou, J. Opt. Soc. Am. A **26,** 350 (2009).

9. G Zhou, J. Opt. Soc. Am. A **25,** 2594 (2008).
10. G. Zhou, Appl. Phys. B **96,** 149 (2009).
11. G. Zhou, Opt. Commun. **283,** 1236 (2010).
12. G. Zhou and X. Chu, Opt. Express **18,** 726 (2010).
13. D. Lu, W. Hu, Y. Zheng, and Z. Yang, Chin. Opt. Lett. **1,** 556 (2003).
14. G. A. Deschamps, Electron. Lett. **7,** 684 (1971).
15. L. B. Felsen, J. Opt. Soc. Am. **66,** 751 (1976).
16. S. Y. Shin and L. B. Felsen, J. Opt. Soc. Am. **67,** 699 (1977).
17. S. R. Seshadri, Opt. Lett. **27,** 998 (2002).
18. S. R. Seshadri, Opt. Lett. **27,** 1872 (2002).
19. S. R. Seshadri, J. Opt. Soc. Am. A **19,** 2134 (2002).
20. S. R. Seshadri, Opt. Lett. **28,** 595 (2003).
21. K. Gao, L. Xu, R. Zheng, G. Chen, H. Zheng, and H. Ming, Chin. Opt. Lett. **8,** 45 (2010).
22. M. A. Bandres and J. C. Gutiérrez-Vega, Opt. Lett. **29,** 2213 (2004).
23. Y. C. Zhang, Y. J. Song, Z. R. Chen, J. H. Ji, and Z. X. Shi, Opt. Lett. **32,** 292 (2007).
24. D. M. Deng and Q. Guo, Opt. Lett. **33,** 1225 (2008).
25. K. Zhu, X. Li, T. Wang, and H. Tang, J. Opt. Soc. Am. A **26,** 2202 (2009).
26. D. M. Deng and Q. Guo, J. Opt. Soc. Am. B **26,** 2044 (2009).
27. P. P. Schmidt, J. Phys. B **9,** 2331 (1976).
28. A. Torre, W. A. B. Evans, O. E. Gawhary, and S. Severini, J. Opt. A: Pure Appl. Opt. **10,** 1464 (2008).
29. G. Zhou, Opt. Express **18,** 4637 (2010).